Molecular Membrane Biology, January–February 2004, 21, 39–50

Taylor & Francis
healthsciences

Mechanistic contributions of residues in the M1 transmembrane domain of the nicotinic receptor to channel gating

Guillermo Spitzmaul, Jeremías Corradi and Cecilia Bouzat*

Instituto de Investigaciones Bioquímicas, UNS-CONICET, Bahía Blanca, Argentina

Summary

The nicotinic receptor (AChR) is a pentamer of homologous subunits with an $\alpha_2\beta\varepsilon\delta$ composition in adult muscle. Each subunit contains four transmembrane domains (M1–M4). Position 15′ of the M1 domain is phenylalanine in α subunits while it is isoleucine in non-α subunits. Given this peculiar conservation pattern, we studied its contribution to muscle AChR activation by combining mutagenesis with single-channel kinetic analysis. AChRs containing the mutant α subunit (αF15′I) as well as those containing the reverse mutations in the non-α subunits (βI15′F, δI15′F, and εI15′F) show prolonged lifetimes of the diliganded open channel resulting from a slower closing rate with respect to wild-type AChRs. The kinetic changes are not equivalent among subunits, the β subunit, being the one that produces the most significant stabilization of the open state. Kinetic analysis of βI15′F AChR channels activated by the low-efficacious agonist choline revealed a 10-fold decrease in the closing rate, a 2.5-fold increase in the opening rate, a 28-fold increase in the gating equilibrium constant of the diliganded receptor, and a significant increased opening in the absence of agonist. Mutations at βI15′ showed that the structural bases of its contribution to gating is complex. Rate-equilibrium linear free-energy relationships suggest an ~70% closed-state-like environment for the β15′ position at the transition state of gating. The overall results identify position 15′ as a subunit-selective determinant of channel gating and add new experimental evidence that gives support to the involvement of the M1 domain in the operation of the channel gating apparatus.

Keywords: acetylcholine, acetylcholine receptor, ion channel, site-directed mutagenesis, patch clamp.

Abbreviations: AChR, nicotinic acetylcholine receptor; ACh, acetylcholine; M1, first transmembrane domain; HEK cells, human embryonic kidney cells; α-BTX, α-bungarotoxin; P_{open}, channel open probability.

Introduction

The nicotinic acetylcholine receptor (AChR) mediates neuromuscular transmission in vertebrates. The adult muscle AChR is a pentamer composed of two α subunits and three non-α subunits, β, δ and ε. All α subunits are characterized by the presence of a pair of adjacent cysteines in the amino-terminal domain. Non-α subunits (lacking the pair of cysteines) have derived from the α subunits during evolution (Ortells and Lunt 1995). Subunit diversity presumably allowed fine tuning of the receptors to respond more appropriately to their different physiological requirements. Two main events are essential for receptor function: agonist recognition and channel gating. How the α and non-α subunits contribute to agonist binding has been described in detail (Prince and Sine 1998). However, the contribution of each subunit to channel gating is not as well understood. Here we study the contribution of residues that are differentially conserved between α and non-α subunits to channel gating.

Each AChR subunit contains an amino-terminal extracellular domain of approximately 210 amino acids, four transmembrane domains (M1–M4), and a short extra-cellular carboxy-terminal tail. The M2 domain of each subunit contributes to the cation-selective channel, and agonist binding triggers its twisting to allow ion flow (Unwin 1995). The disposition and the functional role of the M1 domain are not well known. The M1 domain appears closely associated with the lipid bi-layer and the ion pathway. Labelling experiments with the hydrophobic probe [^{125}I]TID in *Torpedo* AChR identified lipid-exposed residues in αM1, δM1 and γM1 (Blanton and Cohen 1994). Although the labelled residues are located mainly in the middle of the segments, the labelling pattern varies among the different subunits. Akabas and Karlin (1995) and Zhang and Karlin (1997) identified residues in the amino-terminal third of αM1 and βM1 that are accessible to hydrophilic sulfhydryl reagents, thus contributing to the lining of the channel. The exposure of some of these residues changes during gating or desensitization. Again, the exposure pattern varies between the α and β subunits.

A few lines of experimental evidence indicate that M1, together with M2, M3, and M4, contributes to channel gating. Early studies showed that a cysteine located in the middle of M1 and the region surrounding this amino acid are involved in channel gating (Lo *et al.* 1991). Mutations at a highly conserved proline in αM1 produce receptors that gate with a much larger EC_{50} than the normal (England *et al.* 1999). The mutation of an arginine flanking M1 (R209) shifts EC_{50} for ACh and increases the normalized maximal channel activity in *Torpedo* AChR (Tamamizu *et al.* 1995). R209 has been also shown to be involved in either the coupling of agonist binding to channel or the regulation of single-channel kinetics in neuronal α3β4 AChRs (Vicente-Agullo *et al.* 2001). A mutation in αM1 causes a congenital myasthenic syndrome by decreasing the rate of agonist dissociation (Wang *et al.* 1997). A mutation in εM1 has been also shown to be the cause of a congenital myasthenic syndrome mainly due to an increased affinity of ACh for the resting AChR (Croxen *et al.* 2002, Hatton *et al.* 2003). In addition to its contribution to channel gating, M1 has been shown to play an important role in the surface expression of functional α7 AChRs (Vicente-Agullo *et al.* 2001).

*To whom correspondence should be addressed.
e-mail: inbouzat@criba.edu.ar

Molecular Membrane Biology
ISSN 0968-7688 print/ISSN 1464-5203 online © 2004 Taylor & Francis Ltd
http://www.tandf.co.uk/journals
DOI: 10.1080/09687680310001607341

Sequence comparison of subunits reveals several candidate residues in transmembrane domains differentially conserved between α and non-α muscle subunits. By combining site-directed mutagenesis at position 15′ of M1 with single-channel kinetic analysis, we investigated in the present study if this conservation pattern has a functional significance. Our results not only reveal that this pattern represents structures that are important for proper function but also add new experimental evidence that gives support to the involvement of the M1 domain in the operation of the channel-gating apparatus. Although position 15′ is conserved among non-α subunits, its functional role varies among them. The β subunit is the most sensitive to mutations which mainly enhance gating efficiency in the absence and the presence of agonist.

Results

Expression of mutant AChRs

Position 15′ of the M1 domain is phenylalanine in all muscle α subunits and it is isoleucine in non-α subunits (Figure 1).

Given this particular conservation pattern, we studied its contribution to channel gating by combining site-directed mutagenesis and single-channel kinetic analysis. αF15′ was replaced by isoleucine and reverse mutations in β, ε, and δ subunits were carried out. Mutant subunits were co-expressed with the full complement of adult subunit cDNAs in HEK cells. Binding of [^{125}I]α-BTX to cell-surface AChRs showed expression levels ranging from 31% to 126% with respect to those of wild-type AChRs (Figure 2).

Single-channel recordings of M1 mutant AChRs

Single-channel currents activated by 30 μM ACh were recorded from HEK cells expressing the mutant AChRs to study the effects of mutations at position 15′ on gating kinetics. Clusters of events corresponding to activation of a single AChR channel can be clearly recognized at this ACh concentration. Mean open times of AChRs containing the mutant αF15′I, εI15′F, and δI15′F subunits are slightly prolonged with respect to those of wild-type AChRs (Figure 3). However, the substitution of βI15′ by phenylalanine leads to significant changes in the open time distribution. Mean open time increases about 10-fold with respect to that of wild-type AChRs (Figure 3). Mean open times obtained from the corresponding histograms are: wild-type = 0.98 ± 0.15 ms ($n = 10$); αF15′I = 1.57 ± 0.45 ms ($n = 3$); βI15′F = 8.9 ± 1.7 ms ($n = 6$); εI15′F = 2.11 ± 0.11 ($n = 4$); and δI15′F = 1.45 ± 0.18 ms ($n = 9$).

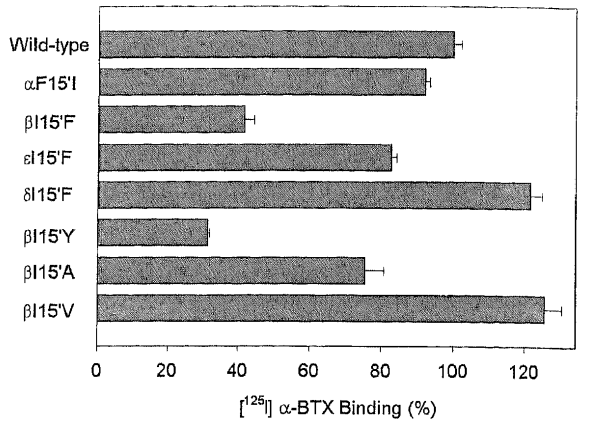

Figure 2. Surface expression of mutant AChRs. HEK 293 cells were transfected with the specified subunit mutated in M1 plus the corresponding wild-type subunits. [^{125}I]α-BTX binding was performed on day 3 after transfection. The total number of binding sites observed for wild-type AChRs corresponds to 100%.

To determine how mutant subunits differentially combined in the pentameric receptor affect open channel duration, cells were transfected with different mutant and wild-type subunits, and the mean open times of the resulting AChRs were compared. As shown in Figure 4, the presence of βI15′F subunit is necessary for producing the maximal changes in the mean open time. Results from the combination of βI15′F with the other mutant subunits suggest that all subunits contribute to the duration of the open state through position 15′. The changes between mutant and wild-type AChRs in the energy for channel closing (Δ(ΔGc)) produced by each subunit are not completely additive. For AChRs containing the five mutant subunits Δ(ΔGc) = −1.62 kcal/mol. However, the addition of the Δ(ΔGc)s calculated for each AChR containing only one mutant subunit results in an energy change of −2.46 kcal/mol.

Closed time histograms of AChRs activated by 30 μM ACh can be well fitted with three or four components. Typically, there is a fast component (20–60 μs), a major intermediate component of about 1 ms, which is sensitive to ACh concentration, and one or two small, variable, slow components that are associated with periods between independent activation episodes (Bouzat *et al*. 2000, Bouzat *et al*. 2002). Closed-time distributions for the αF15′I, εI15′F, and δI15′F AChRs are similar to those for wild-type AChRs but they are

	1′			5′				10′				15′				20′						
α1m	P	L	Y	F	I	V	N	V	I	I	P	C	L	L	F	S	F	L	T	G	L	V	F	Y	L	P
α1h	P	L	Y	F	I	V	N	V	I	I	P	C	L	L	F	S	F	L	T	G	L	V	F	Y	L	P
α1t	P	L	Y	F	V	V	N	V	I	I	P	C	L	L	F	S	F	L	T	G	L	V	F	Y	L	P
β1m	P	L	F	Y	L	V	N	V	I	A	P	C	I	L	I	T	L	L	A	I	F	V	F	Y	L	P
β1h	P	L	F	Y	L	V	N	V	I	A	P	C	I	L	I	T	L	L	A	I	F	V	F	Y	L	P
β1t	P	L	F	Y	I	V	Y	T	I	I	P	C	I	L	I	S	I	L	A	I	L	V	F	Y	L	P
εm	P	L	F	Y	V	I	N	I	I	V	P	C	V	L	I	S	G	L	V	L	L	A	V	F	L	P
δm	P	L	F	Y	I	I	N	I	L	V	P	C	V	L	I	S	F	M	I	N	L	V	F	Y	L	P
γm	P	L	F	Y	V	I	N	I	I	A	P	C	V	L	I	S	S	V	A	I	L	I	Y	F	L	P

Figure 1. Sequence alignment of the M1 transmembrane domain of different subunits.

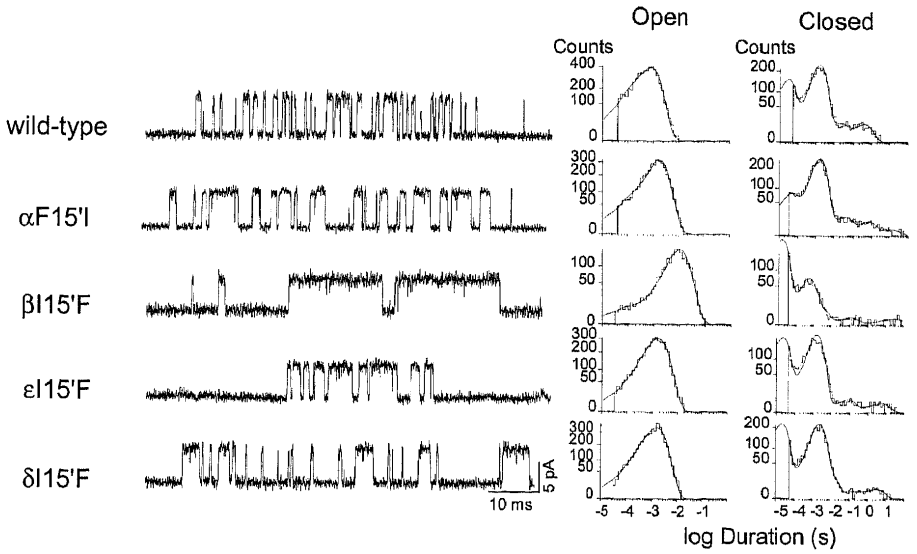

Figure 3. Effects of mutations at position 15′ of M1. *Left*: Channels activated by 30 μM ACh were recorded from HEK cells expressing AChRs containing the mutant αF15′I, βI15′F εI15′F or δI15′F subunits. Currents are displayed at a bandwidth of 9 kHz with channel openings as upward deflections. Membrane potential: −70 mV. *Right*: Open- and closed-time histograms of AChRs carrying the specified mutant subunit.

significantly displaced to briefer durations in the βI15′F AChR (Figure 3).

Probability of channel opening of M1 mutant AChRs

Mean channel open probability within clusters was calculated at a range of ACh concentration to determine the overall consequences of the mutations. For wild-type AChRs, the probability of channel opening within clusters (P_{open}) increases with ACh concentration, reaching its maximum value at about 150 μM and showing an EC_{50} of 38 μM (Figure 5). The curve is displaced to lower ACh concentrations in the βI15′F AChR, showing a 6-fold decrease in the EC_{50} ($EC_{50} = 6$ μM). The Popen curves of αF15′I, δI15′F, and εI15′F are slightly displaced to lower ACh concentrations ($EC_{50} = 28$, 31 and 23 μM for αF15′I, δI15′F, and εI15′F, respectively).

Recordings of AChRs carrying the βI15′F subunit in the absence and presence of low ACh concentrations

When recordings are performed with ACh-free pipette solutions, brief openings corresponding to unliganded AChRs can be detected for both wild-type and βI15′F AChRs. The frequency of spontaneous openings is very low in the wild-type adult AchR, whereas it significantly increases in the mutant AChR (Figure 6(*a*)). For three different patches, the calculated frequency of openings using agonist-free pipette solutions was $0.03 \pm 0.02\ s^{-1}$ and $1.4 \pm 0.6\ s^{-1}$ for wild-type and βI15′F AChRs, respectively. All spontaneous openings

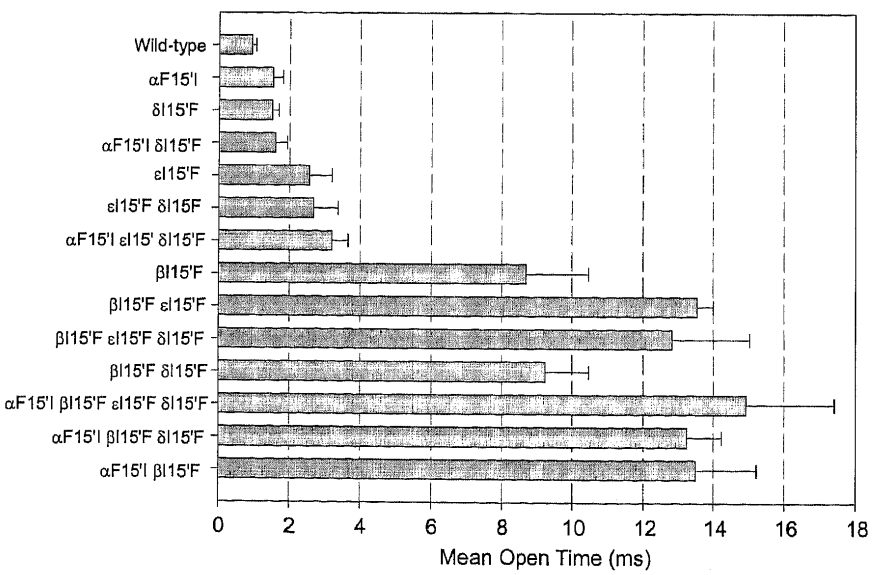

Figure 4. Effects of different combinations of M1 mutant subunits on the mean open time. The mean open time was obtained from AChRs containing the indicated combination of subunits. ACh = 0.5 μM.

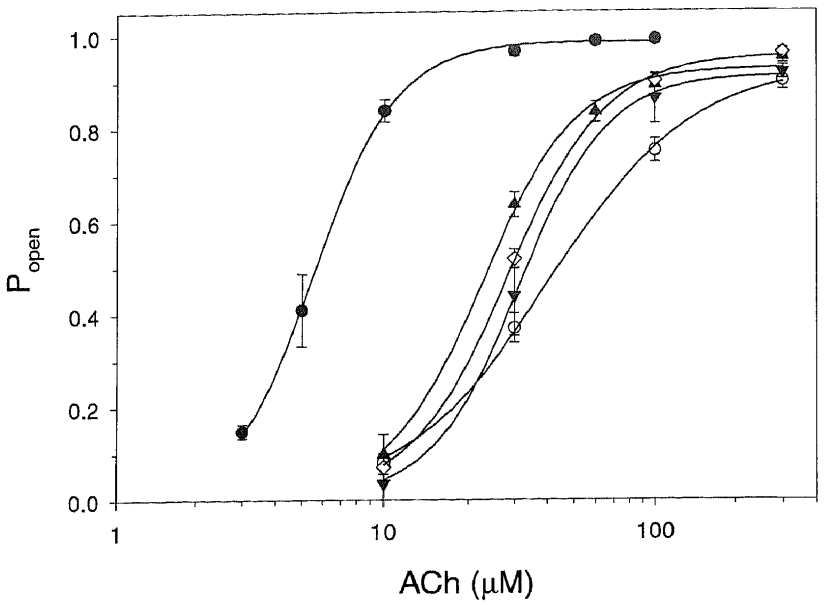

Figure 5. Agonist concentration dependence of the channel open probability. The mean fraction of time the channel is open during a cluster (P_{open}) was experimentally determined at the indicated concentrations of ACh. Each point corresponds to the mean ± SD of at least three patches. The symbols correspond to the following mutant subunits: ○, wild-type; ●, βI15′F; ◇, αF15′I; ▲, εI15′F; ▼, δI15′F.

appear as isolated events (Figure 6(*a*)). The frequency of opening events detected in the absence of ACh is partly affected by the level of expression of the AChRs. Under equal transfection conditions, the expression of βI15′F AChRs is lower than that of wild-type AChRs (see Figure 2). Therefore the increase in the number of spontaneous openings in the mutant AChR is probably under-estimated. However, as it is not possible to calculate the number of channels in each single cell-attached patch, the increase in the frequency of openings cannot be accurately determined.

Thus, in addition to showing increased mean open times, the βI15′F AChR exhibits an unusually high rate of spontaneous opening.

Figure 6(*a*) also shows the open-time distributions in a range of low ACh concentrations for the βI15′F mutant AChR. As shown in this figure, the open distributions at low ACh concentrations can be dissected into three components: (1) the briefest component that corresponds to that observed in the absence of ACh, thus representing openings of unliganded AChRs—the mean open time of this component is 110 ± 30 μs; (2) the longest component which is the main one observed at concentrations higher than 10 μM and which corresponds to diliganded AChRs ($\tau_{on} = 8.7 \pm 1.7$ ms)—the area of this component progressively increases with the increase in ACh concentration, such area being 0.90 ± 0.05 at 10 μM ACh; and (3) an intermediate component of 1.2 ± 0.5 ms which may therefore correspond to openings of monoliganded AChRs (Figure 6(*a*)).

Recordings of βI15′F AChRs at high ACh concentration

We studied the cluster properties of βI15′F AChRs activated by 100 μM ACh (Figure 6(*b*)). Cluster duration histograms show a main component (τ_c) of 133 ± 40 ms and the number of openings per cluster is 13.9 ± 1.6 ($n = 3$). The probability of channel opening within a cluster (P_{open}) is 0.97 at this ACh concentration (see Figure 5). For wild-type AChRs activated by 100 μM ACh, $\tau_c = 46 \pm 10$ ms and the calculated number of openings per cluster = 44.5 ± 9.9. Auerbach and Akk (1998) demonstrated that the value of $(\tau_c P_{open})^{-1}$ is a direct measure of the desensitization rate constant. The estimated value for $(\tau_c P_{open})^{-1}$ is 27 s^{-1} for wild-type and 8 s^{-1} for βI15′F AChRs, thus suggesting that desensitization is slightly slower in mutant than in wild-type AChRs.

Kinetics of AChRs carrying mutations at position 15′ of M1

The observed changes in the open- and closed-time distributions in the M1 mutant AChRs could be due to changes in rate constants underlying either ACh binding or channel gating steps. To identify unequivocally the kinetic steps affected by these mutations, we fitted kinetic schemes to the open- and closed-dwell times. We first used the classical activation scheme (Scheme 1) where two agonists (A) bind to the receptor (R) in the resting state with association rates k_{+1} and k_{+2}, and dissociate with rates k_{-1} and k_{-2}. AChRs occupied by one agonist open with rate β_1 and close with rate α_1, whereas those occupied by two agonist molecules open with rate β_2 and close with rate α_2. At high agonist concentrations (higher than 100 μM ACh), channel blockade is evident and thus the blocked state, A_2B, is included in the scheme. To estimate the set of rate constants, Scheme 1 was fitted to the data by using the QuB software for kinetic analysis (Qin *et al*. 1996).

The predominant peak of the closed-time histograms moves to briefer duration and the open-time histograms remain constant when increasing ACh concentration for wild-type and mutant AChRs (Figure 7). The curves resulting from the analysis superimposed on the experimental open and closed duration histograms at all ACh concentrations for wild-type AChRs (Figure 7). Therefore, Scheme 1 reasonably describes the kinetics of wild-type AChRs. The rate con-

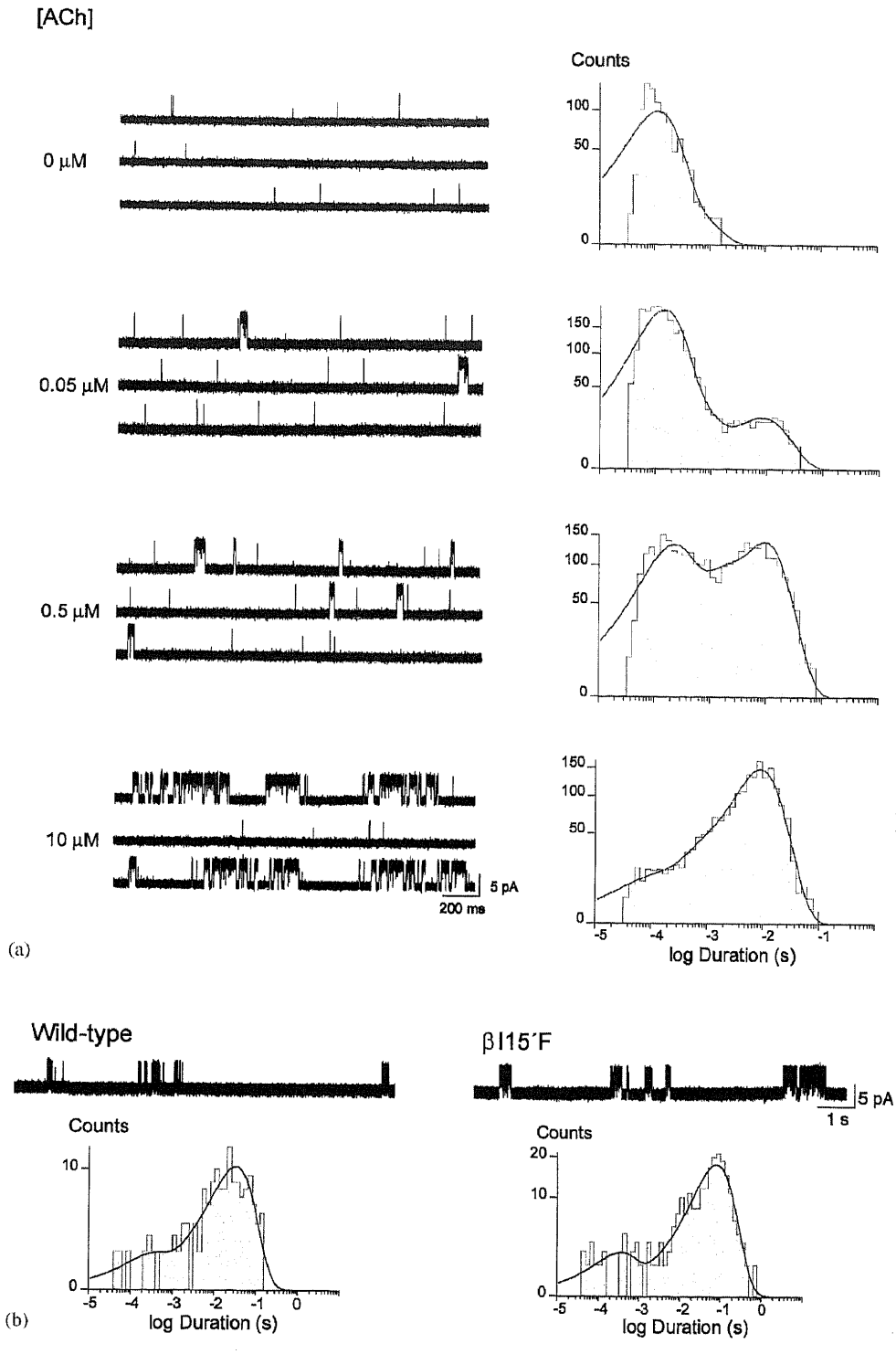

Figure 6. Single-channel recordings of AChRs containing βI15′F mutant subunit in the absence and presence of ACh. (a) Single-channels of βI15′F AChRs recorded in the absence or presence of low ACh concentrations. *Left*: Single-channel currents elicited by the indicated concentrations of ACh. *Right*: Open-time histograms of the corresponding recordings. (b) Single-channels of wild-type and βI15′F AChRs activated by 100 μM ACh. Clusters of wild-type and βI15′F AChRs activated by 100 μM ACh. Cluster duration histograms of the corresponding AChRs are shown below each trace. Membrane potential: −70 mV. Filter: 9 kHz. Channels are shown as upward deflections.

stants obtained for mouse wild-type AChR (Table 1) are similar to those reported previously (Wang *et al*. 1997, Bouzat *et al*. 2000).

Curves resulting from the kinetic analysis of εI15′F (Figure 7) and αF15′I and δI15′F AChRs (data not shown) also fitted correctly the experimental histograms, indicating that Scheme 1 provides a good description of the activation of these mutant AChRs. As shown in Table 1, a slight decrease in the closing rate is observed in these mutant AChRs. For all of them, β_2 had to be constrained to the same value as that of

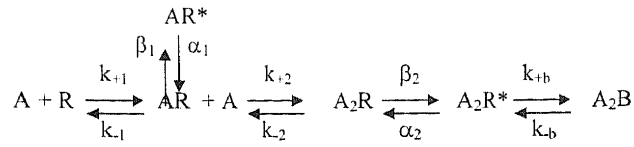

Scheme 1.

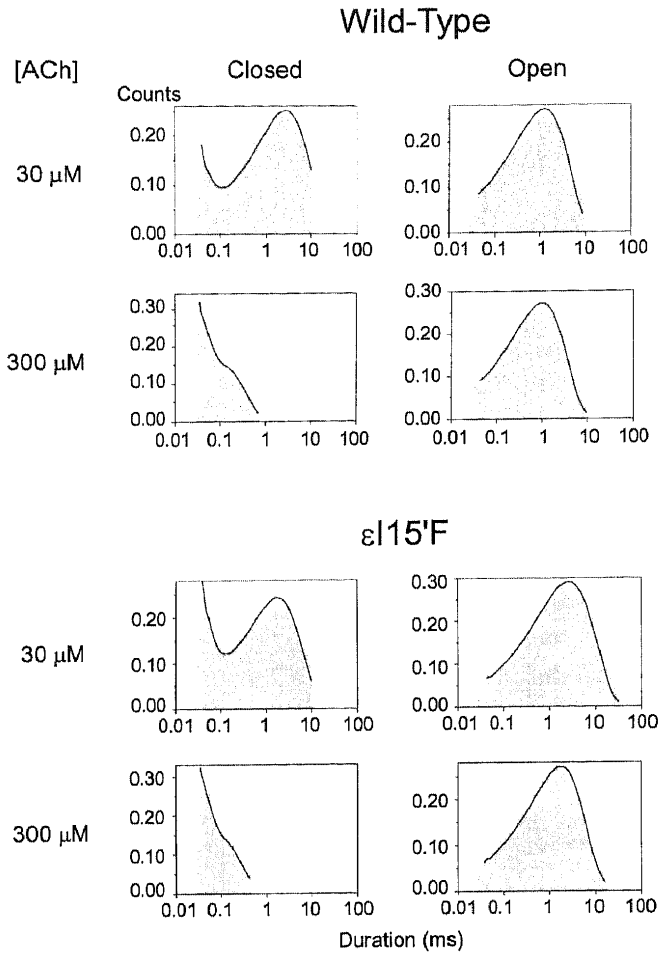

Figure 7. Kinetics of activation of wild-type and εI15′F AChRs. Closed- and open-time histograms corresponding to the selected clusters with the fit for Scheme 1 superimposed. The ordinates correspond to the square root of the fraction of events per bin.

wild-type AChRs to allow the fitting (see Experimental Procedures).

Mutations in the δ and ε subunits could affect agonist binding at only one site. Although no significant changes were observed in agonist association and dissociation rates in these mutant AChRs, we also carried out the kinetic analysis without the constraint of equal association and dissociation rate constants. No significant differences were observed in these rate constants with respect to those similarly calculated for wild-type AChRs (data not shown).

Data corresponding to AChRs containing the βI15′F subunit did not fit Scheme 1. As described before, recordings of the mutant βI15′F AChR channels show a significant number of spontaneous openings and the closed-time distributions are displaced to briefer durations with respect to wild-type AChRs. Both observations could be due to an increase in the opening rate. Because the opening rate constant of wild-type AChRs activated with ACh is at the upper limit of reliable estimation, an increase in this rate cannot be resolved. Choline, an agonist with a very slow opening rate, was therefore used to quantify the changes in the opening- and closing-rate constants introduced by the βI15′F subunit (Zhou *et al*. 1999, Grosman and Auerbach 2000a).

Recordings of βI15′F AChRs activated by choline

At 20 mM choline, openings occur in easily recognizable clusters for both wild-type and mutant AChRs (Figure 8). Open-channel blockade elicited by this high choline concentration appears as a 2-fold reduction in channel amplitude (Grosman and Auerbach 2000a, Bouzat *et al*. 2002, De Rosa *et al*. 2002). The channel currents at −70 mV are: wild-type = 2.24 ± 0.04 pA with 20 mM choline and 5.34 ± 0.16 pA with ACh or choline at concentrations lower than 100 μM; and βI15′F AChRs = 2.40 ± 0.05 pA with 20 mM choline and 5.47 ± 0.07 pA with ACh or choline at concentrations lower than 100 μM. Given that the reduction in channel current is due to open channel blockade (Grosman and Auerbach 2000a) and that such reduction is similar in wild-type and βI15′F AChRs, it is possible to infer that blockade is not affected by the mutation. In this respect, the values for the dissociation equilibrium constant from the pore-blocking site (K_B) at −70 mV, calculated by the decrease in channel current, are 14.5 mM and 15.6 mM for wild-type and βI15′F AChRs, respectively.

For both wild-type and mutant choline-activated AChRs, open-time histograms are well described by a single exponential. The mean open times differ by about an order of magnitude, as observed for ACh (0.58 ± 0.04 ms and 5.30 ± 0.52 ms for wild-type and βI15′F AChRs, respectively). Closed-time histograms for choline-activated AChRs show a main component that corresponds to intra-cluster closings (Figure 8). Mean durations of these components are 20.5 ±

Table 1. Kinetic parameters for mouse wild-type and M1 mutant AChRs. Rate constants are in units of $\mu M^{-1}\ s^{-1}$ for association rate constants and s^{-1} for all others. Values are results of a global fit of Scheme 1 to data obtained over a range of concentration of ACh. Standard errors are shown. Data not showing standard errors have been constrained to allow a good fit.

	k_{+1}	k_{-1}	k_{+2}	k_{-2}	β_1	α_1	β_2	α_2	k_{+b}	k_{-b}
WT	240±10	24320±860	120±5	48640±1720	110±15	2610±310	50000	1610±30	5±1	78000
αF15′I	321±10	28790±1305	160±5	57560±2611	327±49	1611±158	50000	1004±115	5±1	78000
εI15′F	210±5	16310±470	105±3	32200±930	370±40	1160±90	50000	760±15	10±0.5	78000
δI15′F	160±5	17046±740	80±3	34105±1482	255±33	2020±254	50000	950±26	16±0.5	78000

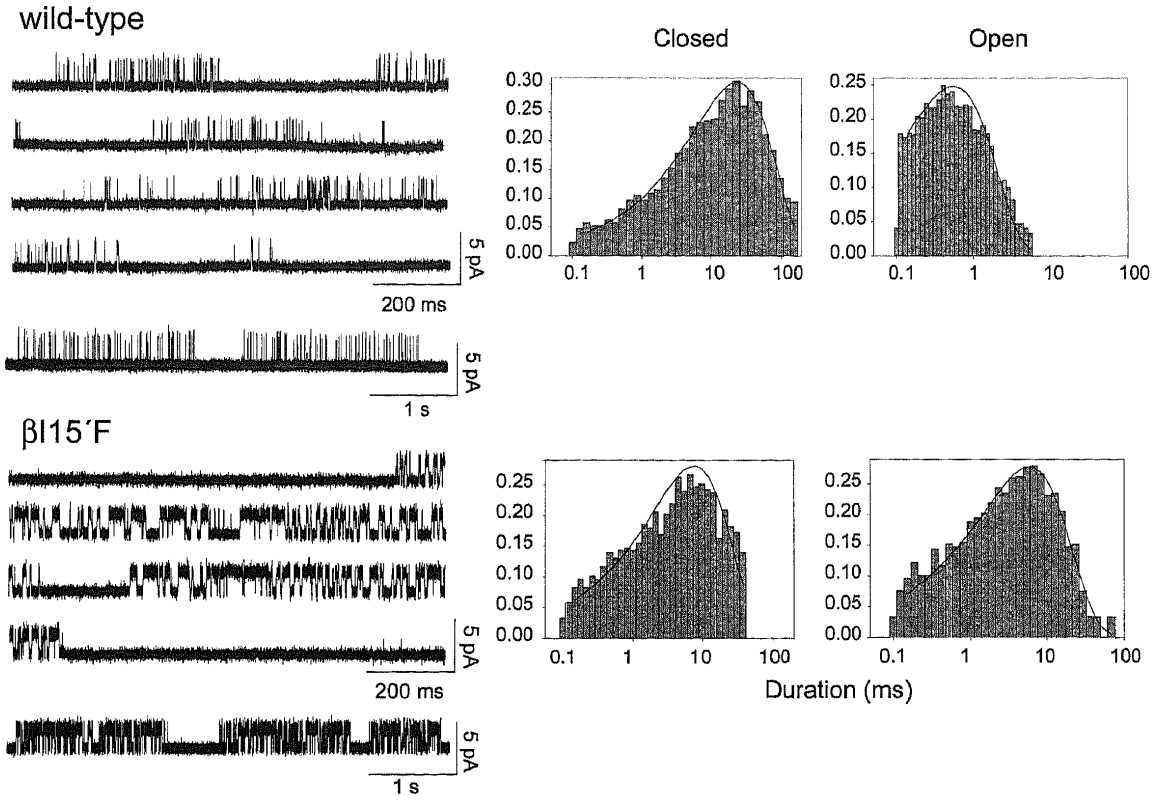

Figure 8. Single-channel currents in the presence of 20 mM choline. *Left*: Channel traces corresponding to AChRs containing wild-type or βI15′F mutant subunits. Continuous recordings are shown in four traces. An additional trace at a different time scale is shown for each AChR. Membrane potential: −70 mV. Openings are shown as upward deflections at a bandwidth of 5 kHz. *Right*: Open- and closed-time histograms with the fit to Scheme 2 superimposed to the experimental histograms. Histograms were constructed with the selected clusters and the ordinates correspond to the square root of the fraction of events per bin.

4.7 ms and 6.8±0.8 ms for wild-type and βI15′F AChRs, respectively.

To analyse the kinetics of channel opening and closing in the presence of 20 mM choline, we fitted Scheme 2 to the closed and open intervals of the selected clusters,

$$A_2R \underset{\alpha_2}{\overset{\beta_2}{\rightleftarrows}} A_2R^*$$

Scheme 2.

Scheme 2 is a subset of Scheme 1 which reduces the kinetics of AChR activity to the closed to open transition because 20 mM choline is a saturating agonist concentration (Grosman and Auerbach 2000a). The resulting estimates for opening and closing rate constants are summarized in Table 2. The estimates reveal that the opening rate increases about 2.5-fold and the closing rate decreases about 10-fold owing to the βI15′F mutation. Consequently, the gating equilibrium constant (θ_2), calculated as β_2/α_2, increases about 28 times in the mutant with respect to wild-type AChRs.

Although αFI15′I, δI15′F and εI15′F AChRs activated by ACh did not show significant changes in the rate constants with respect to wild-type AChRs (Table 1), but given that the opening rate (β_2) had to be constrained in these mutant AChRs, we made recordings at 20 mM choline to confirm that β_2 did not increase in these mutant AChRs. The kinetic analysis carried out for the εI15′F AChR on the basis of Scheme 2 revealed no changes in the opening rate ($\beta_2 = 48\pm10\ s^{-1}$) and slight changes in the closing rate ($\alpha_2 = 910\pm80\ s^{-1}$), in good agreement with the changes observed for activation by ACh (Table 1).

Structural basis of the kinetic effects of βI15′

To study the structural basis of the contribution of βI15′ to channel gating, βI15′ was replaced by other hydrophobic (A and V) and aromatic (Y) amino acids. Single channels activated by 30 μM ACh were then recorded. A concentration of 30 μM was chosen because it is close to the EC_{50} for the adult muscle AChR and, therefore, it is sensitive to changes in activation parameters. The P_{open}, channel mean open duration and mean closed duration were calculated for each cluster within a recording, their distributions were plotted and the mean values were subsequently determined. The values calculated for the mean channel open time, the mean channel closed time, and the probability of opening within clusters are shown in Table 2.

In conclusion, the rank order of the different amino acids at 15′ for enhancing the stabilization of the open state and increasing the Popen is F > A > V > Y ~ I.

Single-channel currents from βI15′A, βI15′V and βI15′Y AChRs activated by 20 mM choline were also recorded

Table 2. Kinetic parameters for wild-type and βI15′ mutant AChRs. For each cluster within a recording at 30 μM ACh, the mean open channel duration, mean closed channel duration and P_{open} was calculated and the distributions were plotted. The mean values and SD obtained from the corresponding distributions are shown. Values of rate constants for choline are results of a global fit of Scheme 2 to data obtained at 20 mM choline. θ_2, calculated as β_2/α_2, is the gating equilibrium constant and was calculated individually for each set of data and then averaged. The data correspond to the mean±SD of at least three different recordings for each condition.

	30 μM ACh			*20 mM choline*		
AChR	Mean open duration (ms)	Mean closed duration (ms)	P_{open}	β_2 (s^{-1})	α_2 (s^{-1})	θ_2
Wild-type	0.93±0.12	1.39±0.20	0.40±0.06	58±10	1982±179	0.029±0.006
βI15′F	9.91±1.67	0.83±0.21	0.96±0.01	149±15	192±18	0.782±0.099
βI15′A	4.05±0.76	1.53±0.54	0.80±0.01	53±8	223±38	0.241±0.034
βI15′V	2.07±0.55	1.15±0.13	0.68±0.06	51±5	827±154	0.063±0.011
βI15′Y	0.87±0.05	1.68±0.22	0.35±0.06	44±5	1512±310	0.030±0.006

(Table 2). As described before, Scheme 2 was fitted to the closed and open intervals to determine the kinetics of channel activation. The results agree with the data obtained in the presence of ACh. The analysis revealed that: (1) βI15′Y AChR is kinetically similar to the wild-type AChR; (2) βI15′A and βI15′V AChRs show decreased closing rates although their opening rates do not increase significantly as in the βI15′F AChRs (Table 2).

Linear free-energy relationships in βM1

We applied LFER analysis to determine the structure of the gating transition state near position β15′ (Grosman and Auerbach 2000a, Grosman *et al*. 2000b). For this analysis, the values calculated for rate (α_2 and β_2) and gating equilibrium (θ_2) constants shown in Table 2 were used. Figure 9 shows Brønsted plots using rates (β_2 or α_2) versus equilibrium constants of the β15′ substitutions. The plots correspond to: $\log \beta_2 = \Phi \log\theta_2 + \text{constant}$ and $\log \alpha_2 = (\Phi - 1) \log\theta_2 + \text{constant}$ (Grosman *et al.* 2000b).

A value for $\Phi = 0.28$ was obtained from the slope of the linear fits. Φ is a measure of the extent to which the transition state resembles the open state in the vicinity of the mutated residue (Cymes *et al*. 2002). This value suggests that the structure of the gating transition state near position 15′ of M1 resembles the closed state, being ~28% similar to that of the open state and ~72% similar to that of the closed state (Grosman *et al*. 2000b). If numbering starts from the C-terminal, βI15′ corresponds then to position 12′ in M1. Interestingly, a Φ value of 0.28 has been calculated for the equivalent position in the M2 segment of the δ subunit (δS12′) (Cymes *et al.* 2002).

Discussion

The contribution to gating of position 15′ of M1 is studied in the present work. This position was particularly chosen because of its conservation pattern. We have recently reported that position 8′ of M3, which shows a similar conservation pattern to that of position 15′ of M1, contributes to the kinetics of AChR activation (De Rosa *et al.* 2002). The results shown in the present study confirm that this profile of conservation marks residues important for AChR function. However, the reason residues were conserved through evolution in such a way still remains intriguing given that the functional roles are not conserved among the different subunits in M3 (De Rosa *et al*. 2002) nor in M1 domain.

There are a few lines of experimental evidence showing the contribution of M1 to channel gating (Lo *et al.* 1991, Engel *et al.* 1996, 2002, Wang *et al.* 1997, Croxen *et al.* 2002, Hatton *et al.* 2003). Our study identifies position 15′ as a subunit-selective determinant of channel gating and adds new experimental evidence that gives support to the involvement of the M1 domain in channel gating. In addition, and to our knowledge, this is the first report that describes in detail the mechanistic contribution of a residue in βM1 to channel gating.

The M1 domain appears closely associated with the ion conducting pathway and the bi-layer, as revealed by substituted cysteine accessibility and labelling by hydrophobic reagents (Blanton and Cohen 1994, Akabas and Karlin 1995). However, position 15′ is neither labelled by TID (Blanton and Cohen 1994) nor is it accessible to polar sulfhydryl-specific reagents when mutated to cysteine (Akabas and Karlin 1995, Zhang and Karlin 1997). Therefore, its location with respect to the lipid bi-layer and pore still remains uncertain.

Our results show that mutations at 15′ profoundly increase the lifetime of the double liganded open channel mainly owing to a decrease in the closing rate. In the β subunit, they also increase significantly the opening rate in the absence of ACh. Prolonged open times and increased spontaneous activity have been described for mutations in other domains, such as the M2 segment (Ohno *et al*. 1995, Engel *et al.* 1996, Milone *et al.* 1997, Grosman and Auerbach 2000b), the M2–M3 linker (Grosman *et al.* 2000a). Most of these mutations have been found associated with slow-channel congenital myasthenic syndromes.

The prolonged apparent mean open time may arise either from an increased opening-rate constant (β_2), or a decreased closing-rate constant (α_2), or a decreased agonist-dissociation rate constant (2k-). Single-channel kinetic analysis was performed in order to determine which of these three alternatives led to the prolonged apparent open intervals. Data from mutations at 15′ of α, ε, and δ subunits could be fitted to the classical activation scheme (Scheme 1), showing slight kinetic changes, which involve mainly a decrease in the closing rate.

Since we could not fit the data from recordings of βI15′F obtained in the presence of ACh to Scheme 1, and because

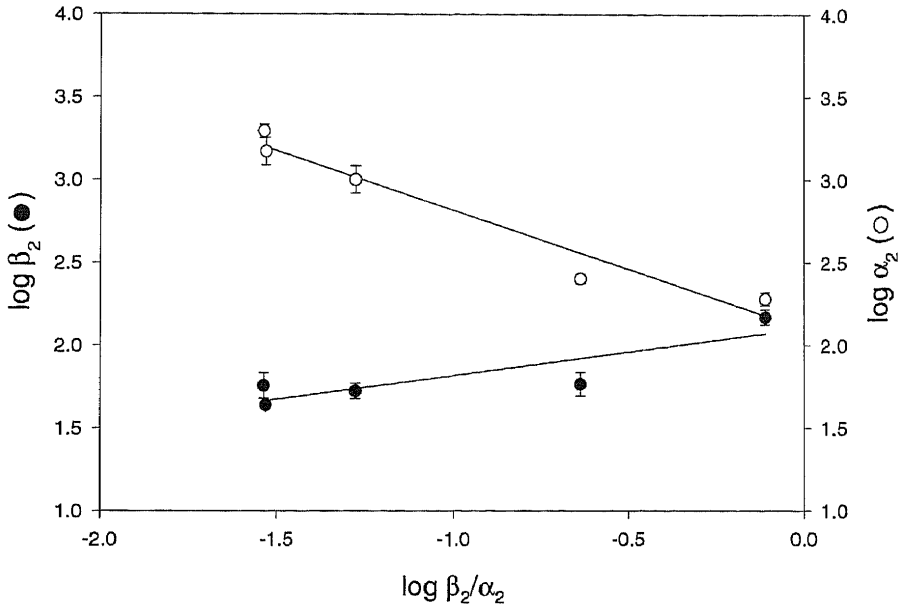

Figure 9. βI15′ LFER analysis. Brønsted plots for βI15′ mutants showing the relationship between the opening rate constant (β_2, ●) or the closing rate constant (α_2, ○) and the diliganded gating equilibrium constant (θ_2). Slopes of the linear fits are: $\Phi = 0.28$ and $\Phi - 1 = -0.71$ for the plots of β_2 vs θ_2 and α_2 vs θ_2, respectively.

the opening rate constant of wild-type AChRs (β_2 in Scheme 1) is at the upper limit of reliable estimation and any increase could therefore not be resolved, choline was used as an agonist (Zhou *et al*. 1999, Grosman and Auerbach 2000a). At a saturating concentration of choline, the kinetics can be reduced to that of the closed to open reaction (Grosman and Auerbach 2000a, Bouzat *et al.* 2002). Given that the opening rate in the choline-activated AChRs is slow, this rate constant can be well measured and thus an increase in such constant can be easily detected. The resulting kinetic analysis confirms that the mean open time is prolonged in the βI15′F owing to a 10-fold decrease in the closing rate. In addition, the mutation also increases the opening rate about 2.5-fold and increases the diliganded gating equilibrium constant (θ_2) about 28-fold. Such increase corresponds to a change in free energy of the gating equilibrium of diliganded AChRs of 2 kcal/mol. Choline activation has been studied for several mutant AChRs causing slow-channel congenital myasthenic syndromes (Zhou *et al*. 1999). For all the mutants, the increase in the θ_2 was due to an increase in the opening rate together with a decrease in the closing rate, as described in the present paper for the βI15′F AChR.

In the absence of agonists, wild-type AChRs open rarely and briefly (Jackson 1986, Engel *et al.* 1996, Milone *et al*. 1997). The frequency of spontaneous openings has been shown to increase as a result of mutations, most of which occur in the M2 domain (Ohno *et al.* 1995, Engel *et al.* 1996, Grosman and Auerbach 2000b). This is the first study documenting an increased spontaneous activity resulting from a mutation in the βM1 domain. Short-lived and isolated openings dominated the unliganded activity in the βI15′F AChR. It has been previously reported that in some M2 mutants, in addition to isolated openings, longer openings grouped in bursts appear in a minor proportion (Grosman and Auerbach 2000b). No spontaneous bursting activity was detected in recordings from βI15′F AChRs.

The mechanistic bases for the kinetic changes described for the βI15′F AChR may be interpreted on the basis of Scheme 3.

In this scheme, resting (R) and active (R*) states of the receptor spontaneously inter-convert in the absence of agonist, and activation is driven by progressive occupancy of the sites together with tighter binding of agonist to the active compared with the resting state. Consistent with its physiological role, the gating reaction of diliganded AChRs is much more favourable than that of unliganded AChRs (Engel *et al.* 2002). Increased spontaneous openings in the βI15′F indicate an increase in the gating equilibrium constant in the absence of agonist (θ_0). From the thermodynamic principle of detailed balance, it follows that $\theta_2 = \theta_0$ ($K_1K_2/K_1{}^*K_2{}^*$). This equation predicts that an increase in θ_2 has to be accompanied by the same increase in θ_0 as long as the affinity ratio of closed and open states is not affected. Given that we cannot have a solid estimate of the number of channels in the patch, it is therefore not possible to have an estimate value for θ_0. Consequently, it is not possible to determine whether the increase in θ_2 observed for the βI15′F activated by choline arises exclusively from an equal increase in θ_0 or whether there is a contribution from a change in the affinity ratio of closed and open states as well. However, given that the β subunit is not involved in agonist binding, it is more

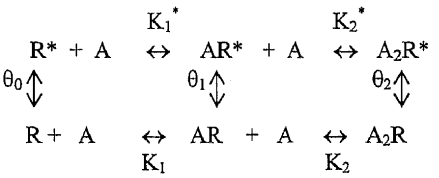

Scheme 3.

probable that the mutation only affects θ_0. A 10-fold increase in the mean open time is observed in the diliganded mutant AChR while there is no significant increase in the mean open time of the unliganded mutant AChR (140 ± 40 μs and 110 ± 30 μs for unliganded wild-type and βI15′F AChRs, respectively). Therefore, the closing rate of unliganded AChRs (α_0) in the βI15′F does not decrease to the same extent as that of the diliganded AChRs (α_2). As a result, the 28-fold increase in the equilibrium constant in the absence of agonist could be mainly due to an increase in the opening rate (βo).

On account of the fact that there is a similar increase in the duration of the open state in the presence of choline and acetylcholine, and that we demonstrated that for choline such increase is mainly due to a decreased closing rate, we can assume that the closing rate in the presence of ACh is $\sim 150\ s^{-1}$ for the βI15′F AChR ($\sim 1500\ s^{-1}$ for wild-type; Bouzat *et al.* 2000). Assuming then that both agonists affect similarly θ_2, the latter will increase also 28 times in the presence of ACh, thus resulting in a value of $\sim 128{,}000\ s^{-1}$ for $\beta^{ACh}_{\beta I15'F}$. Such fast opening rate could not be resolved in our system, which could have been the reason for the unsuccessful performance of the kinetic analysis with this data.

The cluster analysis of βI15′F AChRs activated by 100 μM ACh suggests that the desensitization rate from the biliganded open AChR does not increase with respect to that of wild-type AChRs. By contrast, in most of the M2 mutant AChRs that show an increased gating efficiency, a concomitant increase in desensitization was observed (Engel *et al.* 2002). The reduction in the number of openings per cluster of βI15′F with respect to wild-type AChRs may be explained by means of Scheme 4, in which desensitization is included,

$$C \underset{\alpha_2}{\overset{\beta_2}{\Leftrightarrow}} O \underset{k_{-d}}{\overset{k_{+d}}{\Leftrightarrow}} D$$

Scheme 4.

where C, O and D denote the biliganded closed, open and desensitized conformations. α_2 is about 60 times faster than k_{+d} in the wild-type whereas it is only about 18 times faster in the βI15′F AChR. Therefore, although the desensitization rate seems to be slower in βI15′F AChRs, clusters terminate earlier than those of wild-type AChRs as a result of the increased gating efficiency of the former. This early termination is shown by a decrease in the number of openings per cluster. In the mouse adult AChR, ACh dissociates from the diliganded open receptor at $\sim 24\ s^{-1}$ (Grosman and Auerbach 2001). Owing to the increased gating equilibrium constant in the βI15′F, it is possible that ACh dissociation from the biliganded open state also contributes to the early termination of clusters.

To gain insight into the structural basis of the contribution of 15′ to channel gating, this position in the β subunit was substituted by different amino acids. The results revealed that there is not a clear correlation between the kinetic changes and physicochemical properties of the side chain (volume, polarity, aromaticity). Complex relationships have been previously described for other mutations (Grosman and Auerbach 2000a, De Rosa *et al.* 2002). In addition, there is no strict correlation between the degree of the kinetic change and the decrease in the surface expression of the mutant AChRs. For example, the most significant changes in gating kinetics are observed in the βI15′F, whereas βI15′Y is the one that produces the largest decrease in the level of surface expression. As a result, the effects observed in the present study seem not to be due to a global perturbation but rather to a local perturbation involving position 15′.

To probe the closed-like structure versus the open-like structure of β15′ at the gating transition state, the correlation between rate and equilibrium constant of the gating reaction for different amino acid substitutions was analysed. Although our analysis did not include a large number of amino acids, this correlation seems to be quite linear. This linearity indicates that the closed and open forms of the diliganded AChRs are connected either by a single reaction pathway or by a set of parallel pathways of similar fractional Φ-values (Grosman *et al.* 2000). The Φ value of 0.28 thus obtained suggests an intermediate structure that is neither totally open ($\Phi = 1$) nor totally closed ($\Phi = 0$) as well as a more closed-state-like environment for the β15′ position at the transition state of gating. From the cytoplasmic end of the transmembrane segments, βI15′ occupies the equivalent position to δS12' in M2 (Cymes *et al.* 2002). Both positions show similar Φ values, suggesting that the structure of the transition state is similar at these two residues located in different transmembrane domains. A Φ value of 0.83 was determined for αN217, which corresponds to position 7' of M1 and it is therefore located closer to the N-terminal end of M1 than βI15′ (Grosman *et al.* 2000). Assuming that the M1 segments of the different subunits behave similarly, the comparison of the Φ values of αN217 and βI15′ shows that the conformational wave of channel gating in M1 proceeds from the extra-cellular to the intra-cellular region. This is in agreement with data reported by Cymes *et al.* (2002) showing that the rearrangement of the extra-cellular portion may precede that of the intra-cellular part of δM2 during opening.

Finally, abnormal activation of AChR has been shown to underlie congenital myasthenic syndromes (CMS). A few mutations in M1 associated with CMS have been reported to date (Engel *et al.* 2002, Hatton *et al.* 2003). Consequently, if mutations naturally occurred at position 15′ of M1 they could lead to CMSs and their clinical consequences could depend on the subunit affected as well as on the structural change.

Experimental procedures

Construction of mutant subunits

Mouse muscle cDNAs were sub-cloned into the cytomegalovirus-based expression vector pRBG4 (Sine 1993). Mutant subunits were constructed using the QuikChange™ Site-Directed mutagenesis kit (Strategene, Inc., TX). Restriction mapping and DNA sequencing confirmed all constructs.

Expression of AChR

HEK293 cells were transfected with α, β, δ, and ε cDNA subunits (wild-type or mutants using calcium phosphate precipitation at a subunit ratio of 2:1:1:1 for α:β:δ:ε respectively, essentially as previously described (Bouzat *et al.* 1994, 1998). For transfections,

cells at 40–50% confluence were incubated for 8–12 h at 37°C with the calcium phosphate precipitate containing the cDNAs in DMEM plus 10% foetal bovine serum. Cells were used for single-channel measurements 1 or 2 days after transfection. Expression levels of surface AChRs were measured by ^{125}I-α-Bungarotoxin ([^{125}I]α-BTX) binding. Cells were incubated with 10 nM [^{125}I]α-BTX for 60 min at room temperature. Non-specific binding was determined in the presence of 20 mM carbamylcholine.

Patch-clamp recordings

Recordings were obtained in the cell-attached configuration (Hamill *et al.* 1981) at a membrane potential of −70 mV and at 20°C. The bath and pipette solutions contained 142 mM KCl, 5.4 mM NaCl, 1.8 mM $CaCl_2$, 1.7 mM $MgCl_2$ and 10 mM HEPES (pH 7.4). Patch pipettes were pulled from 7052 capillary tubes (Garner Glass, CA) and coated with Sylgard (Dow Corning, Midland, MI). Pipette resistance ranged from 5 to 7 MΩ. Acetylcholine (ACh) at final concentrations of 0.05–300 μM was added to the pipette solution. To measure spontaneous openings, we first detected the presence of AChR channels with a pipette containing 1 μM ACh and then we used a new electrode to make recordings from the same cell with ACh-free solution. On this way, we can ensure that the cell expresses AChRs and we avoid possible contamination of the electrode with ACh.

Single channel currents were recorded using an Axopatch 200 B patch-clamp amplifier (Axon Instruments, Inc., CA), digitized at 5 μs intervals with the PCI-6111E interface (National Instruments, Austin, TX), recorded to the hard disk of a computer using the program Acquire (Bruxton Corporation, Seattle, WA), and detected by the half-amplitude threshold criterion using the program TAC 4.0.10 (Bruxton Corporation, Seattle, WA) at a final bandwidth of 10 kHz. Open- and closed-time histograms were plotted using a logarithmic abscissa and a square root ordinate (Sigworth and Sine 1987) and fitted to the sum of exponential functions by maximum likelihood using the program TACFit (Bruxton Corporation, Seattle, WA).

Data of AChRs activated by 20 mM choline were recorded at a membrane potential of −70 mV and analysed at a bandwidth of 5 kHz to avoid detection of some blockages that could be resolved at 10 kHz. In this manner, channel kinetics can be reduced to those of the closed to open reaction (Grosman and Auerbach 2000a, De Rosa et al. 2002). Owing to open-channel block, AChRs activated by 20 mM choline show a 50% reduction in channel amplitude (De Rosa et al. 2002).

Open probability within clusters (P_{open}) was determined experimentally at each ACh concentration by calculating the mean fraction of time that the channel is open within a cluster.

Kinetic analysis

Kinetic analysis was performed as described before (Wang *et al.* 1997, Bouzat *et al.* 2000, 2002). The analysis was restricted to clusters of channel openings, each reflecting the activity of a single AChR. Clusters were identified as a series of closely spaced events preceded and followed by closed intervals longer than a critical duration (τ_{crit}). This duration was taken as the point of intersection of the predominant closed component and the succeeding one in the closed-time histogram. The predominant closed duration component becomes shorter with the increase of agonist concentration. Consequently, we assume that this component reflects the set of transitions between unliganded closed and diliganded open states. To minimize errors in assigning cluster boundaries, we analysed only recordings from patches with low channel activity in which both components are clearly differentiated from one another. Only clusters containing more than 10 openings were considered for further analysis. In addition, clusters showing double openings were rejected.

For each recording, kinetic homogeneity was determined by selecting clusters on the basis of their distribution of mean open duration, mean closed duration and open probability (Wang *et al.* 1997, Bouzat *et al.* 2000, 2002). Typically, the distributions contained an approximately Gaussian dominant component and minor contributions of clusters with different properties. Clusters showing mean open channel durations, mean closed channel durations and open probability values within two standard deviations of the mean of the major component were selected. Typically, more than 80% of the clusters were selected and only the non-Gaussian appendages were omitted (Bouzat *et al.* 2000). Mean values obtained from distributions of open probability, mean open channel duration and mean closed channel duration of clusters do not change significantly after the selection procedure (Bouzat *et al.* 2000). In addition, comparison of closed- and open-time histograms before and after selection indicates that the selected clusters are representative of the predominant population of AChR in the patch (Bouzat *et al.* 2000).

The resulting open and closed intervals from single patches at several ACh concentrations were analysed according to kinetic schemes using an interval-based full-likelihood algorithm (www.qub.buffalo.edu; QuB suite, State University of New York, Buffalo). Briefly, the program allows simultaneous fitting of recordings at different agonist concentrations and estimates the rate constants using a maximum likelihood method that corrects for missed events (Qin *et al.* 1996). The dead time was 30 μs. Probability density functions of open and closed durations were calculated from the fitted rate constants and instrumentation dead time and superimposed on the experimental dwell time histogram as described by Qin *et al.* (1996). Calculated rates were accepted only if the resulting probability density functions correctly fitted the experimental open- and closed-duration histograms.

We used an ACh concentration range from 1 to 100 μM for the βI15′F AChR, and from 10 to 300 μM for wild-type, αF15′I, εI15′F, and δI15′F AChRs. These ranges were chosen on the basis of the Popen values. For wild-type and some mutant AChRs activated by ACh the opening rate of the diliganded AChR, β_2 in Scheme 1, had to be constrained to its previously determined value (Sine *et al.* 1995, Wang *et al.* 1997, Salamone *et al.* 1999) because brief closings due to gating and channel blocking become indistinguishable at high ACh concentrations (Wang *et al.* 1997, Salamone *et al.* 1999, Bouzat *et al.* 2000). When β_2 was allowed to vary freely, the program did not converge to a well-defined set of rate constants and β_2 approached a value of about 100000 s^{-1} (Salamone *et al.* 1999, Bouzat *et al.* 2000). Also, association and dissociation rate constants were assumed to be equal at both binding sites (Akk *et al.* 1996, Wang *et al.* 1997, Salamone *et al.* 1999, Bouzat *et al.* 2000). Rate constants are shown with standard deviations (SD).

For kinetic analysis of AChRs activated by choline, we fitted dwell times from the selected clusters to a kinetic scheme containing only one open and one closed state given that 20 mM choline is a saturating agonist concentration (Grosman and Auerbach 2000a). Owing to the fast blockade of choline at 20 mM, the mean duration of the apparent openings would be about 2-fold longer than that observed at low concentrations of the agonist. As the single channel amplitude was reduced to similar extents in wild-type and mutant AChR, the prolongation of the openings is expected to be the same for all tested constructs. Thus, all closing rate constants obtained may be underestimated by a factor ≤ 2 (Grosman and Auerbach 2000a, De Rosa *et al.* 2002).

Acknowledgements

This work was supported by grants from Ministerio de Salud de la Nación, Universidad Nacional del Sur, Agencia Nacional de Promoción Científica y Tecnológica (PICT 98 01-03586), Fundación Antorchas, Third World Academy of Sciences (TWAS), International Society of Neuroscience (ISN) to CB; and FIC grant (1R03 TW01185-01) to Dr. Steven M. Sine (Mayo Foundation, MN, USA) and CB.

Note added in proof

After submission of this manuscript, an atomic model of the closed pore of the Torpedo AChR was reported by Miyazawa *et al.* (Miyazawa, A., Fujiyoshi, Y. and Unwin, N., 2003, Structure and gating mechanism of acetylcholine receptor pore, *Nature*, **423**, 949–955, 2003). Interestingly, position 15′ of M1 may interact with M2, and this potential interaction may affect gating.

References

Akabas, M. H. and Karlin, A., 1995, Identification of acetylcholine receptor channel-lining residues in the M1 segment of the alpha-subunit. *Biochemistry*, **34**, 12496–12500.

Akk, G., Sine, S. and Auerbach, A., 1996, Binding sites contribute unequally to the gating of mouse nicotinic alpha D200N acetylcholine receptors. *Journal of Physiology*, **496**, 185–196.

Auerbach, A. and Akk, G., 1998, Desensitization of mouse Nicotinic Acetylcholine Receptor channels. A two-gate mechanism. *Journal of General Physiology*, **112**, 181–197.

Blanton, M. P. and Cohen, J. B., 1994, Identifying the lipid–protein interface of the Torpedo nicotinic acetylcholine receptor: secondary structure implications. *Biochemistry*, **33**, 2859–2872.

Bouzat, C., Bren, N. and Sine, S. M., 1994, Structural basis of the different gating kinetics of fetal and adult acetylcholine receptors. *Neuron*, **13**, 1395–1402.

Bouzat, C., Roccamo, A. M., Garbus, I. and Barrantes, F. J., 1998, Mutations at lipid-exposed residues of the acetylcholine receptor affect its gating kinetics. *Molecluar Pharmacology*, **54**, 146–153.

Bouzat, C., Barrantes, F. and Sine, S., 2000, Nicotinic receptor fourth transmembrane domain: hydrogen bonding by conserved threonine contributes to channel gating kinetics. *Journal of General Physiology*, **115**, 663–672.

Bouzat, C., Gumilar, F., Esandi, M. C and Sine, S. M., 2002, Subunit-selective contribution to channel gating of the M4 domain of the nicotinic receptor. *Biophysics Journal*, **82**, 1920–1929.

Croxen, R., Hatton, C., Shelley, C., Brydson, M., Chauplannaz, G., Oosterhuis, H., Vincent, A., Newsom-Davis, J., Colquhoun, D. and Beeson, D., 2002, Recessive inheritance and variable penetrance of slow-channel congenital myasthenic syndromes. *Neurology*, **59**, 162–168.

Cymes, G. D., Grosman, C. and Auerbach, A., 2002, Structure of the transition state of gating in the acetylcholine receptor channel pore: a Φ-value analysis. *Biochemistry*, **41**, 5548–5555.

De Rosa, M. J., Rayes, D., Spitzmaul, G. and Bouzat, C., 2002, Nicotinic receptor M3 transmembrane domain: position 8′ contributes to channel gating. *Molecular Pharmacology*, **62**, 406–414.

Engel, A. G., Ohno, K., Milone, M., Wang, H. L., Nakano, S., Bouzat, C., Pruitt, J. N., Hutchinson, D. O., Brengman, J. M., Bren, N., Sieb, J. P. and Sine, S. M., 1996, New mutations in acetylcholine receptor subunit genes reveal heterogeneity in the slow-channel congenital myasthenic syndrome. *Human Molecular Genetics*, **5**, 1217–1227.

Engel, A. G., Ohno, K. and Sine, S. M., 2002, The spectrum of congenital myasthenic syndromes. *Molecular Neurobiology*, **26**, 347–367.

England, P. M., Zhang, Y., Dougherty, D. A. and Lester, H. A., 1999, Backbone mutations in transmembrane domains of a ligand-gated ion channel: implications for the mechanism of gating. *Cell*, **96**, 89–98.

Grosman, C. and Auerbach, A., 2000a, Asymmetric and independent contribution of the second transmembrane segment 12′ residues to diliganded gating of acetylcholine receptor channels: a single-channel study with choline as the agonist. *Journal of General Physiology*, **115**, 637–651.

Grosman, C. and Auerbach, A., 2000b, Kinetic, mechanistic, and structural aspects of unliganded gating of acetylcholine receptor channels: a single-channel study of second transmembrane segment 12′ mutants. *Journal of General Physiology*, **115**, 621–635.

Grosman, C. and Auerbach, A., 2001, The dissociation of acetylcholine from open nicotinic receptor channels. *Proceedings of the National Academy of Sciences (USA)*, **98**, 14102–14107.

Grosman, C., Salamone, F. N., Sine, S. M. and Auerbach, A., 2000a, The extracellular linker of muscle acetylcholine receptor channels is a gating control element. *Journal of General Physiology*, **116**, 327–340.

Grosman, C., Zhou, M. and Auerbach, A., 2000b, Mapping the conformational wave of acetylcholine receptor channel gating. *Nature*, **403**, 773–776.

Hamill, O. P., Marty, A., Neher, E., Sakmann, B. and Sigworth, F. J., 1981, Improved patch-clamp techniques for high-resolution current recording from cells and cell-free membrane patches. *Pflügers Archiv*, **391**, 85–100.

Hatton, C. J., Shelley, C., Brydson, M., Beeson, D. and Colquhoun, D., 2003, Properties of the human muscle nicotinic receptor, and of the slow-channel myasthenic syndrome mutant (L221F, inferred from maximum likelihood fits. *Journal of Physiology*, **547**, 729–760.

Jackson, M. B., 1986, Kinetics of unliganded acetylcholine receptor channel gating. *Biophysics Journal*, **49**, 663–672.

Lo, D. C., Pinkham, J. L. and Stevens, C. F., 1991, Role of a key cysteine residue in the gating of the acetylcholine receptor. *Neuron*, **6**, 31–40.

Milone, M., Wang, H. L., Ohno, K., Fukudome, T., Pruitt, J. N., Bren, N., Sine, S. M. and Engel, A. G., 1997, Slow-channel myasthenic syndrome caused by enhanced activation, desensitization, and agonist binding affinity attributable to mutation in the M2 domain of the acetylcholine receptor alpha subunit. *Journal of Neuroscience*, **17**, 5651–5665.

Ohno, K., Hutchinson, D. O., Milone, M., Brengman, J. M., Bouzat, C., Sine, S. M. and Engel, A. G., 1995, Congenital myasthenic syndrome caused by prolonged acetylcholine receptor channel openings due to a mutation in the M2 domain of the epsilon subunit. *Proceedings of the National Academy of Sciences (USA)*, **92**, 758–762.

Ortells, M. O. and Lunt, G. G., 1995, Evolutionary history of the ligand-gated ion-channel superfamily of receptors. *Trends in Neurosciences*, **18**, 121–127.

Prince, R. J. and Sine, S. M., 1998, The ligand binding domains of the nicotinic acetylcholine receptor. In F. J. Barrantes, ed. *The Nicotinic Acetylcholine Receptor: Current Views and Future Trends* (Springer Verlag, Austin, TX), pp. 31–59.

Qin, F., Auerbach, A. and Sachs, F., 1996, Estimating single-channel kinetic parameters from idealized patch-clamp data containing missed events. *Biophysics Journal*, **70**, 264–280.

Salamone, F. N., Zhou, M. and Auerbach, A., 1999, A re-examination of adult mouse nicotinic acetylcholine receptor channel activation kinetics. *Journal of Physiology*, **516**, 315–330.

Sigworth, F. J. and Sine, S. M., 1987, Data transformations for improved display and fitting of single-channel dwell time histograms. *Biophysics Journal*, **52**, 1047–1054.

Sine, S. M., 1993, Molecular dissection of subunit interfaces in the acetylcholine receptor: identification of residues that determine curare selectivity. *Proceedings of the National Academy of Sciences (USA)*, **90**, 9436–9440.

Sine, S. M., Ohno, K., Bouzat, C., Auerbach, A., Milone, M., Pruitt, J. N. and Engel, A. G., 1995, Mutation of the acetylcholine receptor alpha subunit causes a slow- channel myasthenic syndrome by enhancing agonist binding affinity. *Neuron*, **15**, 229–239.

Tamamizu, S., Todd, A. P. and McNamee, M. G., 1995, Mutations in the M1 region of the nicotinic acetylcholine receptor alter the sensitivity to inhibition by quinacrine. *Cell Molecular Neurobiology*, **15**, 427–438.

Unwin, N., 1995, Acetylcholine receptor channel imaged in the open state. *Nature*, **373**, 37–43.

Vicente-Agullo, F., Rovira, J. C., Sala, S., Sala, F., Rodriguez-Ferrer, C., Campos-Caro, A., Criado, M. and Ballesta, J. J., 2001, Multiple roles of the conserved key residue arginine 209 in neuronal nicotinic receptors. *Biochemistry*, **40**, 8300–8306.

Wang, H. L., Auerbach, A., Bren, N., Ohno, K., Engel, A. G. and Sine, S. M., 1997, Mutation in the M1 domain of the acetylcholine receptor alpha subunit decreases the rate of agonist dissociation. *Journal of General Physiology*, **109**, 757–766.

Zhang, H. and Karlin, A., 1997, Identification of acetylcholine receptor channel-lining residues in the M1 segment of the beta-subunit. *Biochemistry*, **36**, 15856–15864.

Zhou, M., Engel, A. G. and Auerbach, A., 1999, Serum choline activates mutant acetylcholine receptors that cause slow channel congenital myasthenic syndromes. *Proceedings of the National Academy of Sciences (USA)*, **96**, 10466–10471.

Received 25 April 2003; and in revised form 12 June 2003.